Journal of Solid State Chemistry **160**, 415–420 (2001)
doi:10.1006/jssc.2001.9258, available online at http://www.idealibrary.com on IDEAL®

$Ca_3Ni_8In_4$—An Ordered Noncentrosymmetric Variant of the $BaLi_4$ Type

Vasyl' I. Zaremba,* Ihor R. Muts,* Yaroslav M. Kalychak,* Rolf-Dieter Hoffmann,†
and Rainer Pöttgen†,[1]

Inorganic Chemistry Department, Ivan Franko National University of Lviv, Kyryla and Mephodiya Street 6, 79005 Lviv, Ukraine; and †Department Chemie, Ludwig-Maximilians-Universität München, Butenandtstrasse 5-13 (Haus D), D-81377 Munich, Germany

Received February 28, 2001; in revised form April 21, 2001; accepted May 25, 2001; published online July 26, 2001

The title compound was synthesized by reacting the elements in an arc-melting apparatus under purified argon and subsequent annealing at 870 K. $Ca_3Ni_8In_4$ was investigated using X-ray diffraction on both powders and single crystals: $P6_3mc$, $a = 898.9(1)$ pm, $c = 752.2(2)$ pm, $wR2 = 0.0591$, 327 F^2 values, and 35 parameters. This structure is an ordered, noncentrosymmetric variant of the $BaLi_4$ type. The nickel and indium atoms build a complex three-dimensional $[Ni_8In_4]$ polyanion in which the calcium atoms fill distorted hexagonal channels. To a first approximation the formula may be written as $(3\ Ca^{2+})^{6+}$ $[Ni_8In_4]^{6-}$. Within the polyanion the Ni1, Ni3, and Ni4 atoms form one-dimensional cluster units which extend in the *c* direction while the Ni2 atoms have only indium neighbors in a distorted tetrahedral coordination. The Ni–Ni distances in the cluster range from 241 to 266 pm. The cluster units are surrounded and interconnected by indium atoms. The group–subgroup relation from centrosymmetric $BaLi_4$ to noncentrosymmetric $Ca_3Ni_8In_4$ is presented. Chemical bonding in $Ca_3Ni_8In_4$ and the structural relation with $Lu_3Co_{7.77}Sn_4$, $Ca_3Au_{6.61}Ga_{4.39}$, and Co_2Al_5 is briefly discussed. © 2001 Academic Press

Key Words: **intermetallic indium compounds; crystal structure; polyanion.**

INTRODUCTION

The ternary systems alkaline earth metal (*AE*)–transition metal (*T*)–indium have been intensively investigated in recent years (1–17) with respect to crystal chemistry, chemical bonding, and physical properties. The degree of In–In bonding in the ternary compounds $AE_xT_yIn_z$ seems to depend strongly on the indium content as well as on the electron count. In the equiatomic *AET*In indides (1, 6–8, 14) with TiNiSi-type structure (18) the In–In distances vary from 327 (CaRhIn) to 349 pm (CaAuIn). The shorter In–In distance in CaRhIn clearly indicates that electrons from In–In bonding states are taken by the more electron-poor transition metals to fill their *d* states. This lowers the occupancy of antibonding indium states leading to shorter In–In distances.

In–In bonding already becomes more important in $Sr_2Rh_2In_3$ (15), which crystallizes with its own structure type. The In–In distances within and between the In–In zig-zag chains of the pronounced two-dimensional $[Rh_2In_3]$ polyanion range from 303 to 318 pm. Three-dimensional indium substructures are observed in the indides $AETIn_2$ with $MgCuAl_2$ (19) or $CaRhIn_2$ (14) type structure. These indium networks are derived from the well-known structure of hexagonal diamond, lonsdaleite (20). The In–In distances within the distorted tetrahedral networks cover the large range from 309 pm in $CaPtIn_2$ (10) to 391 pm in $BaPtIn_2$ (17). In these compounds the modulation of the In–In distances again clearly depends on the electron count as well as on the size of the alkaline earth atoms.

If the indium content is further increased, the distorted tetrahedral networks collapse. In the structures of $CaTIn_4$ (T = Ni, Cu, Rh, Pd, Ir) (4, 16) with $YNiAl_4$ (21) or $LaCoAl_4$ (22) type distorted *bcc*-like indium cubes similar to those in elemental indium (20) occur. However, in the ternary compounds the In–In distances are generally shorter than in elemental indium. Chemical bonding in such structures is discussed in (16, 23–26).

When it comes to the transition-metal-rich parts of the systems alkaline earth metal (*AE*)–transition metal (*T*)–indium, only some compounds with copper as transition metal component have been investigated, i.e., $CaCu_4In$ (3, 5), $CaCu_{6.1}In_{5.9}$ (4, 5), and $CaCu_8In_3$ (4). In contrast to the indium-rich indides, these intermetallics show a huge degree of Cu–Cu bonding, e.g., condensed $Cu_{4/4}$ tetrahedra (Cu–Cu 258–261 pm) in $CaCu_4In$ (3, 5) or condensed planar $Cu_{4/4}$ units (Cu–Cu 269–271 pm) in $CaCu_6In_6$ (5). All of these Cu–Cu bond lengths are close to the Cu–Cu distance in *fcc* copper where each copper atom has 12 neighbors at 256 pm (20).

We have now extended our investigations with respect to the nickel-rich compounds. Herein we report on the

---

[1] To whom correspondence should be addressed.

syntheses and structure determination of $Ca_3Ni_8In_4$, a new compound with a pronounced one-dimensional nickel cluster, which was discovered by us for the first time during an investigation of the isothermal section of the phase equilibria of the Ca–Ni–In system at 870 K.

EXPERIMENTAL

Starting materials for the synthesis of $Ca_3Ni_8In_4$ were ingots of calcium ($>99.8\%$, redistilled), electrolytic nickel pieces ($>99.9\%$), and indium tear drops ($>99.9\%$). The sample was prepared by arc-melting the elements in the atomic ratio Ca:Ni:In = 3:8:4 on a water-cooled copper crucible under an argon atmosphere. The argon was purified before over titanium sponge (900 K), silica gel, and molecular sieves. Given the high volatility of calcium in comparison to nickel and indium, the starting charge contained an excess of about 2% calcium. The sample was arc-melted three times in order to achieve homogeneity. After the melting procedures, the deviation from the required composition was less than 1 wt%.

The compact polycrystalline sample was subsequently sealed in an evacuated quartz glass ampoule and annealed at 870 K in a muffle furnace over a period of three months. The annealing temperature was controlled electronically. After the annealing procedure the sample was quenched in ice water. Polycrystalline pieces of $Ca_3Ni_8In_4$ are light gray with metallic lustre; powders are dark gray. $Ca_3Ni_8In_4$ is stable in moist atmosphere over several weeks.

The reaction product was characterized through its X-ray powder pattern (Dron–3M powder diffractometer, Cu$K\alpha$ radiation) using 5N silicon ($a = 543.07$ pm) as an internal standard. The pattern could completely be indexed with a hexagonal cell. The lattice parameters (see Table 1) were obtained from a least-squares fit of the X-ray powder data. To ensure correct indexing, the observed pattern was compared with a calculated pattern (27) taking the atomic positions from the structure refinement. The lattice parameters of the single crystal were in good agreement with those derived from the power data.

The qualitative and quantitative EDX (energy dispersive analyses of X-rays) analyses performed on the investigated single crystal using a Philips EDX 515 scanning electron microscope gave the following results (Ca:Ni:In in atomic percentages): 17.8:55.5:26.7, close to the ideal ratio of 20.0:53.3:26.7. No impurities were observed in the microprobe analysis.

Single crystal intensity data were collected at room temperature by use of a four-circle diffractometer (CAD4) with graphite monochromatized Mo$K\alpha$ (71.073 pm) radiation and a scintillation counter with pulse height discrimination. The scans were taken in the $\omega/2\theta$ mode and an empirical absorption correction was applied on the basis of psi-scan data. All relevant details concerning the data collection are listed in Table 1.

TABLE 1
Crystal Data and Structure Refinement for $Ca_3Ni_8In_4$

Empirical formula	$Ca_3Ni_8In_4$
Molar mass (g/mol)	1049.20
Space group, Z	$P6_3mc$, 2
Pearson symbol	hP30
Unit cell dimensions	$a = 898.9(1)$ pm
(powder data)	$c = 752.2(2)$ pm
	$V = 0.5264$ nm^3
Calculated density (g/cm^3)	6.62
Crystal size (μm^3)	$45 \times 55 \times 65$
Transmission ratio (max/min)	1.65
Absorption coefficient (mm^{-1})	23.9
$F(000)$	960
θ range for data collection	2° to 30°
Range in hkl	$-12 \leq h \leq 4, \pm 12, \pm 10$
Total no. of reflections	2225
Independent reflections	327 ($R_{\mathrm{int}} = 0.0876$)
Reflections with $I > 2\sigma(I)$	314 ($R_{\mathrm{sigma}} = 0.0399$)
Data/restraints/parameters	327/1/35
Goodness-of-fit on F^2	1.139
Final R indices $[I > 2\sigma(I)]$	$R1 = 0.0232$
	$wR2 = 0.0585$
R indices (all data)	$R1 = 0.0248$
	$wR2 = 0.0591$
Extinction coefficient	0.0064(5)
Flack parameter	0.01(7)
Largest differential peak and hole	1.81 and -1.00 e/Å^3

RESULTS AND DISCUSSION

Structure Determination and Refinement

Irregularly shaped single crystals of $Ca_3Ni_8In_4$ were isolated from the annealed sample and examined on a RKV-86 camera (Mo$K\alpha$ radiation) by Laue and rotation photographs. The reciprocal layers $hk0$ and $h0l$ showed the hexagonal Laue class $6/mmm$. The systematic extinctions (hhl only observed for $l = 2n$) led to space groups $P6_3/mmc$, $P6_3mc$, and $P\bar{6}2c$. The noncentrosymmetric space group $P6_3mc$ (No. 186) was found to be correct during structure refinement. The relevant crystallographic data are listed in Table 1.

The starting atomic parameters were deduced from an automatic interpretation of direct methods with Shelxs-97 (28). The structure was then successfully refined using Shelxl-97 (29) (full-matrix least-squares on F^2) with anisotropic atomic displacement parameters for all atoms. As a check for the correct composition and the correct site assignment, the occupancy parameters were refined in separate series of least-squares cycles along with the displacement parameters. All sites were fully occupied within two standard deviations (Table 2) and in the final cycles the ideal occupancy parameters were assumed again. A final

TABLE 2
Atomic Coordinates and Isotropic Displacement Parameters (pm^2) for $Ca_3Ni_8In_4$

Atom	Wyckoff position	Occupancy	*x*	*y*	*z*	U_{eq}
Ca	6*c*	1.01(1)	0.4704(1)	− x	0.2341(4)	116(5)
Ni1	2*a*	1.00(1)	0	0	0.0017(4)	75(5)
Ni2	2*b*	1.00(1)	$\frac{2}{3}$	$\frac{1}{3}$	0.4255(7)	136(5)
Ni3	6*c*	1.01(1)	0.09855(8)	2x	0.2495(4)	98(3)
Ni4	6*c*	1.02(1)	0.1604(1)	2x	0.5621(3)	113(3)
In1	2*b*	1.01(1)	$\frac{1}{3}$	$\frac{2}{3}$	0.5745(3)	116(3)
In2	6*c*	1.00(1)	0.83060(4)	2x	0.4297(1)	97(2)

Note. U_{eq} is defined as one third of the trace of the orthogonalized U_{ij} tensor. The occupancy parameters were refined in a separate series of least-squares cycles. In the final cycles the ideal occupancies were assumed.

difference Fourier syntheses was flat (Table 1). The correct absolute structure was ensured through refinement of the Flack parameter (30, 31). The positional parameters and interatomic distances of the refinement are listed in Tables 2 and 3. Listings of the observed and calculated structure factors are available.[2]

Crystal Chemistry and Chemical Bonding

Besides the indium-rich compounds $CaNiIn_2$ (2) and $CaNiIn_4$ (4), $Ca_3Ni_8In_4$ is the third intermetallic compound in the ternary system calcium–nickel–indium for which the crystal structure was determined. The crystal chemistry of these intermetallics is quite different. $CaNiIn_2$ (2) with $MgCuAl_2$-type structure may be considered as a nickel-filled variant of the Zintl phase $CaIn_2$ (32) and $CaNiIn_4$ (4) contains distorted *bcc*-like indium cubes. Recent electronic structure calculations (10, 14, 16) have shown that In–In bonding plays the important role in these structures. This is totally different in metal-rich $Ca_3Ni_8In_4$, where the shortest In–In contacts at 370 pm may not be considered as bonding. From a geometrical point of view, the $CaNiIn_2$ (2) and $CaNiIn_4$ (4) structures can be considered as built up from two planar layers stacked one upon the other along the short lattice parameter. This is generally observed for ternary indides of the rare earth and 3*d* metals (33). In this context, the $Ca_3Ni_8In_4$ structure may be considered as a multilayer structure along the *c* axis.

A view of the $Ca_3Ni_8In_4$ structure along the hexagonal axis is presented in Fig. 1. The nickel atoms Ni1, Ni3, and Ni4 build a one-dimensional cluster unit which extends along the *c* axis. The Ni–Ni distances within this part of the structure range from 241 to 266 pm, close to the Ni–Ni distance of 249 pm in *fcc* nickel (20). The In2 atoms are located around the nickel cluster at Ni–In contacts ranging from 255 to 277 pm, similar to the Ni–In bond lengths in $CaNiIn_2$ (2) and $CaNiIn_4$ (4). The shorter Ni–In distances compare well with the sum of Pauling's single bond radii of 265 pm for nickel and indium (34). The cluster units are condensed via the Ni2 and In1 atoms which are located on the 2*b* positions 1/3, 2/3, *z* and 2/3, 1/3, *z*. These two atoms have a slightly distorted terahedral near neighbor coordination: Ni2 with three In2 at 255 pm and one In1 at 264 pm, while In1 has one closer Ni2 neighbor at 264 pm and three Ni4 at 269 pm. As expected from the low indium content of our compound, there occur no bonding In–In contacts. The In1–In2 distance of 370 pm is the shortest in the structure. In view of the tetragonal body-centered indium structure ($a = 325.2$, $c = 494.7$ pm) (20) where each indium atom has four nearest neighbors at 325 pm and eight further neighbors at 338 pm, the In1–In2 distance in $Ca_3Ni_8In_4$ is certainly not bonding.

TABLE 3
Interatomic Distances (pm), Calculated with the Lattice Parameters Taken from X-Ray Powder Data of $Ca_3Ni_8In_4$

Ca:	1 Ni2	315.3(6)
	2 Ni4	316.8(2)
	2 Ni3	318.3(1)
	2 In2	319.7(2)
	1 In1	328.3(3)
	2 In2	329.6(3)
	1 In1	333.3(3)
	1 Ni2	337.8(4)
	2 Ni4	348.5(3)
	2 Ca	369.6(4)
	2 Ca	387.2(1)
Ni1:	3 Ni3	241.4(3)
	3 Ni3	244.0(3)
	3 Ni4	253.8(2)
	3 In2	269.3(1)
Ni2:	3 In2	255.3(1)
	1 In1	264.0(5)
	3 Ca	315.3(6)
	3 Ca	337.8(4)
Ni3:	1 Ni1	241.4(3)
	1 Ni1	244.0(3)
	1 Ni4	254.0(4)
	2 Ni4	259.7(2)
	1 In2	264.7(3)
	2 Ni3	265.8(2)
	2 In2	266.5(2)
	2 Ca	318.3(1)
Ni4:	1 Ni1	253.8(2)
	1 Ni3	254.0(4)
	2 Ni3	259.7(2)
	1 In1	269.4(2)
	2 In2	275.6(1)
	1 In2	276.9(2)
	2 Ca	316.8(2)
	2 Ca	348.5(3)
In1:	1 Ni2	264.0(5)
	3 Ni4	269.4(2)
	3 Ca	328.3(3)
	3 Ca	333.3(3)
	3 In2	369.5(2)
In2:	1 Ni2	255.3(1)
	1 Ni3	264.7(3)
	2 Ni3	266.5(2)
	1 Ni1	269.3(1)
	2 Ni4	275.6(1)
	1 Ni4	276.9(2)
	2 Ca	319.7(2)
	2 Ca	329.6(3)
	1 In1	369.5(2)

Note. All distances shorter than 520 pm (Ca–Ca), 480 pm (Ca–Ni), 415 pm (Ni–In, In–In), and 370 pm (Ni–Ni) are listed.

In view of the Pauling electronegativities (35) Ca: 1.00, Ni: 1.91, and In: 1.78, the calcium atoms as the least electronegative component of $Ca_3Ni_8In_4$ have most likely transferred their valence electrons to the nickel and indium atoms. This leads to strong Ni–Ni and Ni–In bonding. The according electron counting can be (approximately) written as $(3\ Ca^{2+})^{6+}[Ni_8In_4]^{6-}$, emphasizing the covalent bonding within the $[Ni_8In_4]^{6-}$ polyanion.

A view in Pearson's Handbook (36) readily showed the structure type $BaLi_4$ (37) with Pearson code hP30. In the

---

[2] Details may be obtained from: Fachinformationszentrum Karlsruhe, D-76344 Eggenstein-Leopoldshafen (Germany), by quoting the Registry No's. CSD-411733.

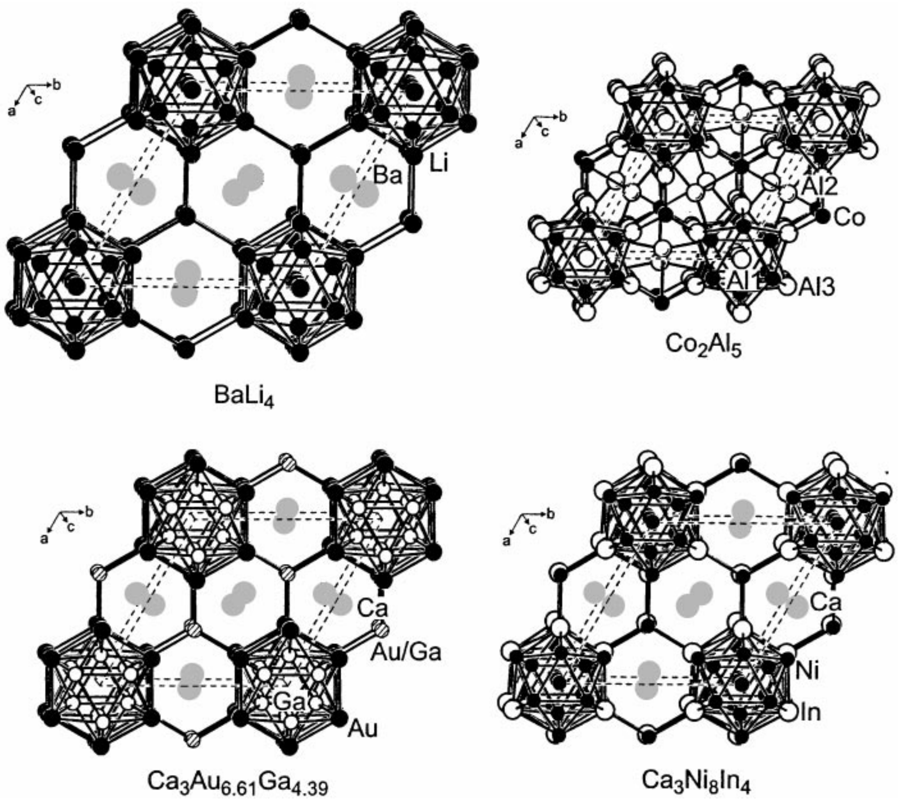

FIG. 1. View of the crystal structures of $Ca_3Ni_8In_4$, $BaLi_4$, Co_2Al_5, and $Ca_3Au_{6.61}Ga_{4.39}$ along the hexagonal axis. Calcium, nickel(cobalt, gold), and indium(lithium, aluminum, gallium) atoms are drawn as gray, filled, and open circles, respectively. The Au/Ga mixed occupied site in the $Ca_3Au_{6.61}Ga_{4.39}$ structure is drawn as hatched circle. The three-dimensional $[Ni_8In_4]$ and $[Au_{6.61}Ga_{4.39}]$ networks for the calcium compounds are emphasized while the Co–Co and Co–Al bonds are drawn for Co_2Al_5. The lithium atoms in $BaLi_4$ are connected for better comparison with the other structures. These connections are not necessarily chemical bonds.

initial stage of the structure determination we started with the centrosymmetric space group $P6_3/mmc$ (No. 194), assuming the $BaLi_4$ type. The 4*f* and 12*k* sites showed mixed occupancies with about 50% nickel and 50% indium. This was a clear indication for lowering of the space group symmetry. We switched to space group $P6_3mc$, a *translationengleiche* subgroup of index 2 of $P6_3/mmc$. Refinement of the structure in this noncentrosymmetric group allowed a complete ordering of the nickel and indium atoms. The structure of $Ca_3Ni_8In_4$ might therefore be considered as a noncentrosymmetric ordered variant of $BaLi_4$. In Fig. 2 we present the group–subgroup relation of both structure types in the concise and compact Bärnighausen formalism (38, 39).

The same structure was recently also observed for the stannide $Lu_3Co_{7.77}Sn_4$ (40, 41), however, one cobalt position showed significant defects. Furthermore, the $Lu_3Co_{7.77}Sn_4$ structure was refined with the opposite absolute structure, when compared with $Ca_3Ni_8In_4$. The stannides $RECo_3Sn$ (RE = Y, Sm, Gd–Yb) (41, 42) were ascribed to the $BaLi_4$ type (space group $P6_3/mmc$) on the basis of X-ray powder data, however, with a mixed Co/Sn occupancy on the 12*k* site.

A cutout of the cluster unit is shown in Fig. 3 as a view perpendicular to the 6_3 screw axis. The Ni1 atoms have distorted icosahedral coordination by nine nickel and three indium atoms. These distorted Frank–Kasper polyhedra (43, 44) are condensed via common triangular faces formed by the Ni3 atoms. This coordination type is typically observed for *d*-metal atoms. The calcium atoms as the largest component in $Ca_3Ni_8In_4$ have coordination number (CN) 18. Both indium sites have CN 13. These coordination spheres might be considered as icosahedra with one additional atom.

The $Ca_3Ni_8In_4$ structure shows some similarities with the structure of Co_2Al_5 (45) and the recently determined structure of the gallide $Ca_3Au_{6.61}Ga_{4.39}$ (46). These structures are shown together with the $BaLi_4$ structure in Fig. 1. As mentioned above, the $Ca_3Ni_8In_4$ structure is a noncentrosymmetric ordered variant of $BaLi_4$. Co_2Al_5 and $Ca_3Au_{6.61}Ga_{4.39}$ both have the Pearson code hP28, however, these structures are also related to the $BaLi_4$ type. In

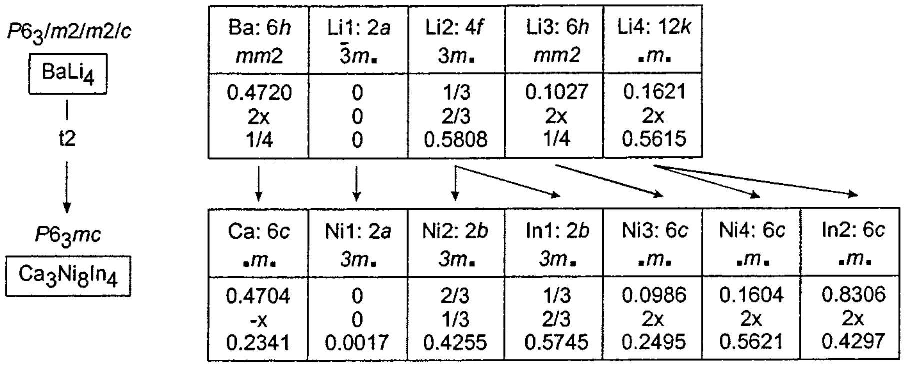

Ba: 6*h* *mm*2	Li1: 2*a* $\bar{3}m.$	Li2: 4*f* 3*m*.	Li3: 6*h* *mm*2	Li4: 12*k* .*m*.
0.4720 2x 1/4	0 0 0	1/3 2/3 0.5808	0.1027 2x 1/4	0.1621 2x 0.5615

Ca: 6*c* .*m*.	Ni1: 2*a* 3*m*.	Ni2: 2*b* 3*m*.	In1: 2*b* 3*m*.	Ni3: 6*c* .*m*.	Ni4: 6*c* .*m*.	In2: 6*c* .*m*.
0.4704 -x 0.2341	0 0 0.0017	2/3 1/3 0.4255	1/3 2/3 0.5745	0.0986 2x 0.2495	0.1604 2x 0.5621	0.8306 2x 0.4297

FIG. 2. Group–subgroup relation in the Bärnighausen formalism (38, 39) for the structures of $BaLi_4$ and $Ca_3Ni_8In_4$. The index of the *translationengleiche* transition (t2) and the evolution of the atomic parameters is given.

$CoAl_5$, the cluster unit is similar to $BaLi_4$ and $Ca_3Ni_8In_4$; however, only two cobalt atoms are located on the 2/3, 1/3, 3/4 2*b* site instead of four atoms with free *z* parameters in $BaLi_4$ (4 Li2) and $Ca_3Ni_8In_4$ (2 Ni2 + 2 In1). In the $Ca_3Au_{6.61}Ga_{4.39}$ structure on the other hand, the icosahedral clusters are empty (Fig. 3).

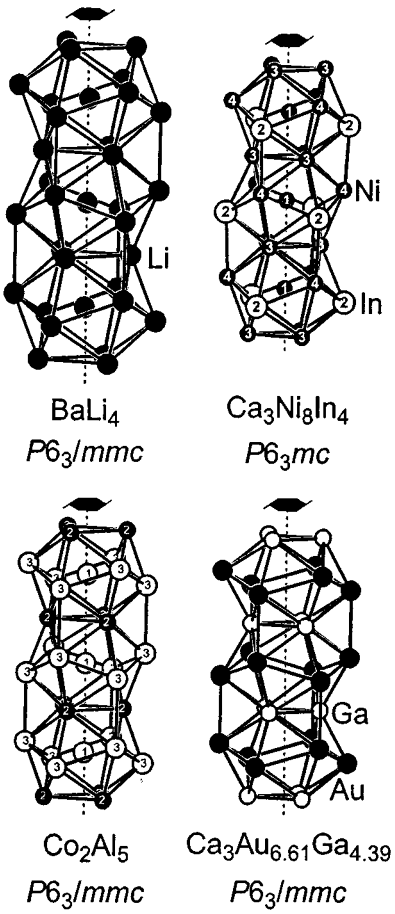

FIG. 3. Cutouts of the cluster units in the structures of $Ca_3Ni_8In_4$, $BaLi_4$, Co_2Al_5, and $Ca_3Au_{6.61}Ga_{4.39}$ which extend along the hexagonal axis. The position of the 6_3 screw axis and some relevant atom designations are also shown.

ACKNOWLEDGMENTS

We are grateful to the Fonds der Chemischen Industrie and the Deutsche Forschungsgemeinschaft for financial support.

REFERENCES

1. S. Cirafici, A. Palenzona, and F. Canepa, *J. Less-Common Met.* **107,** 179 (1985).
2. V. I. Zaremba, O. Ya. Zakharko, Ya. M. Kalychak, and O. I. Bodak, *Dopov. Akad. Nauk. Ukr. RSR, Ser. B* 45 (1987).
3. G. Cordier and C. Röhr, *Z. Kristallogr.* **197,** 314 (1991).
4. L. V. Sysa and Ya. M. Kalychak, *Crystallogr. Rep.* **38,** 278 (1993).
5. L. V. Sysa and Ya. M. Kalychak, *Inorg. Mater.* **30,** 725 (1994).
6. K. Dascoulidou-Gritner and H. U. Schuster, *Z. Anorg. Allg. Chem.* **620,** 1151 (1994).
7. G. Nuspl, K. Polborn, J. Evers, G. A. Landrum, and R. Hoffmann, *Inorg. Chem.* **35,** 6922 (1996).
8. D. Kußmann, R.-D. Hoffmann, and R. Pöttgen, *Z. Anorg. Allg. Chem.* **624,** 1727 (1998).
9. L. V. Sysa, Ya. M. Kalychak, Ya. V. Galadzhun, V. I. Zaremba, L. G. Akselrud, and R. V. Skolozdra, *J. Alloys Compd.* **266,** 17 (1998).
10. R.-D. Hoffmann, R. Pöttgen, G. A. Landrum, R. Dronskowski, B. Künnen, and G. Kotzyba, *Z. Anorg. Allg. Chem.* **625,** 789 (1999).
11. R.-D. Hoffmann and R. Pöttgen, *Z. Anorg. Allg. Chem.* **625,** 994 (1999).
12. R.-D. Hoffmann, R. Pöttgen, C. Rosenhahn, B. D. Mosel, B. Künnen, and G. Kotzyba, *J. Solid State Chem.* **145,** 283 (1999).
13. R.-D. Hoffmann, U. Ch. Rodewald, and R. Pöttgen, *Z. Naturforsch.* **54b,** 38 (1999).
14. R.-D. Hoffmann and R. Pöttgen, *Z. Anorg. Allg. Chem.* **626,** 28 (2000).
15. R.-D. Hoffmann, D. Kußmann, and R. Pöttgen, *Int. J. Inorg. Mater.* **2,** 135 (2000).
16. R.-D. Hoffmann and R. Pöttgen, *Chem. Eur. J.* **6,** 600 (2000).
17. R.-D. Hoffmann and R. Pöttgen, *Chem. Eur. J.* **7,** 382 (2001).
18. C. B. Shoemaker and D. P. Shoemaker, *Acta Crystallogr.* **18,** 900 (1965).
19. B. Aronsson, M. Bäckman, and S. Rundqvist, *Acta Chem. Scand.* **14,** 1001 (1960).
20. J. Donohue, "The Structures of the Elements." Wiley, New York, 1974.

21. R. M. Rykhal', O. S. Zarechnyuk, and Ya. P. Yarmolyuk, *Sov. Phys. Crystallogr.* **17,** 453 (1972).
22. R. M. Rykhal', O. S. Zarechnyuk, and Ya. P. Yarmolyuk, *Dopov. Akad. Nauk Ukr. RSR*, *Ser. A* **39,** 265 (1977).
23. U. Häussermann, S. I. Simak, R. Ahuja, B. Johansson, and S. Lidin, *Angew. Chem.* **111,** 2155 (1999).
24. U. Häussermann, S. I. Simak, R. Ahuja, and B. Johansson, *Angew. Chem. Int. Ed.* **39,** 1246 (2000).
25. J. K. Burdett, "Chemical Bonding in Solids," Oxford University Press, New York, 1995. p. 270.
26. R.-D. Hoffmann, R. Pöttgen, V. I. Zaremba, and Ya. M. Kalychak, *Z. Naturforsch.* **55b,** 834 (2000).
27. K. Yvon, W. Jeitschko, and E. Parthé, *J. Appl. Crystallogr.* **10,** 73 (1977).
28. G. M. Sheldrick, "SHELXS-97," Program for the Solution of Crystal Structures, University of Göttingen, 1997.
29. G. M. Sheldrick, "SHELXL-97," Program for Crystal Structure Refinement, University of Göttingen, 1997.
30. H. D. Flack and G. Bernadinelli, *Acta Crystallogr. Sect. A: Found Crystallogr.* **55,** 908 (1999).
31. H. D. Flack and G. Bernadinelli, *J. Appl. Crystallogr.* **33,** 1143 (2000).
32. A. Iandelli, *Z. Anorg. Allg. Chem.* **330,** 221 (1964).
33. Ya. M. Kalychak, *J. Alloys Compd.* **262–263,** 341 (1997).
34. L. Pauling, "The Nature of the Chemical Bond and the Structures of Molecules and Crystals." Cornell University Press, Ithaca, NY, 1960.
35. J. Emsley, "The Elements." Oxford University Press, Oxford, 1989.
36. P. Villars and L. D. Calvert, "Pearson's Handbook of Crystallographic Data for Intermetallic Phases," second edition. American Society for Metals, Materials Park, OH, 1991. [Desk Edition, 1997]
37. F. E. Wang, F. A. Kanda, C. F. Miskell, and A. J. King, *Acta Crystallogr.* **18,** 24 (1965).
38. H. Bärnighausen, *Commun. Math. Chem.* **9,** 139 (1980).
39. H. Bärnighausen and U. Müller, "Symmetriebeziehungen zwischen den Raumgruppen als Hilfsmittel zur straffen Darstellung von Strukturzusammenhägen in der Kristallchemie." University of Karlsruhe and University Gh. Kassel, Germany, 1996.
40. R. Skolozdra, B. García-Landa, D. Fruchart, D. Gignoux, J. L. Soubeyroux, and L. Akselrud, *J. Alloys Compd.* **235,** 210 (1996).
41. R. V. Skolozdra, Stannides of rare-earth and transition metals, *in* "Handbook on the Physics and Chemistry of Rare Earths" (K. A. Gschneidner Jr. and L. Eyring, Eds.), Vol. 24, Chap. 164, pp. 399–517. Elsevier, Amsterdam, 1997.
42. J. Mudryk, D. Fruchart, D. Gignoux, L. P. Romaka, and R. V. Skolozdra, *J. Alloys Compd.* **312,** 9 (2000).
43. F. C. Frank and J. S. Kasper, *Acta Crystallogr.* **11,** 184 (1958).
44. F. C. Frank and J. S. Kasper, *Acta Crystallogr.* **12,** 483 (1959).
45. J. B. Newkirk, P. J. Black, and A. Damjanovic, *Acta Crystallogr.* **14,** 532 (1961).
46. D. Kußmann, R.-D. Hoffmann, and R. Pöttgen, *Z. Anorg. Allg. Chem.*, in press.